

Supplementary Information

Light Controlled Oxidation by Supramolecular Zn(II) Schiff-base Complexes

Christian Laube^{a,b}, Josef Taut^a, Jonas Kretzschmar^d, Stefan Zahn^a, Wolfgang Knolle^a, Steve Ullman^d, Axel Kahnt^a, Berthold Kersting^d, and Bernd Abel^{a,c}

a) Leibniz Institute for Surface Engineering (IOM), Department Functional Surfaces, D-04318 Leipzig, Germany

b) Department of Chemistry, University of California, Berkeley, California 94720, USA

c) Wilhelm-Ostwald-Institute of Physical und Theoretical Chemistry, Universität Leipzig, Linnéstraße 2, D-04103 Leipzig, Germany

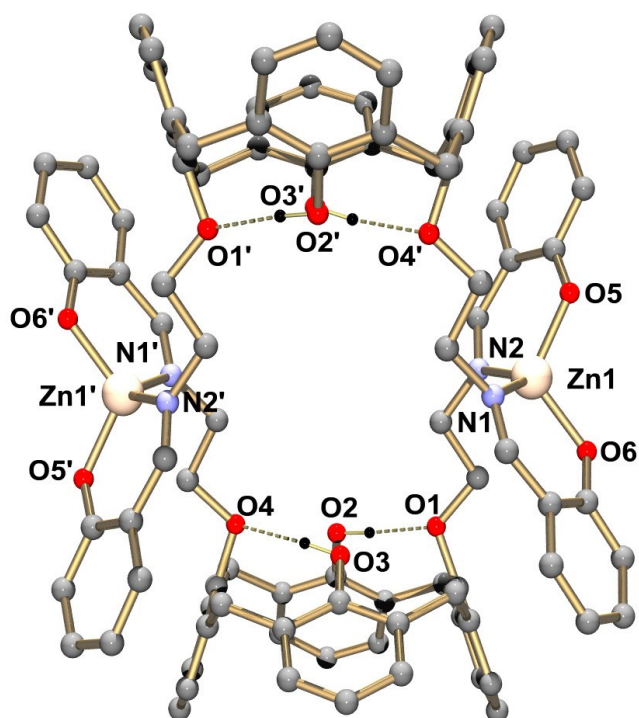
d) Institute of Inorganic Chemistry, University Leipzig, Johannisallee 29, 04103 Leipzig, Germany

Table of Contents

Description of the Crystal Structure of ZnL1	3
Investigations on the Photoinduced Isomerisation of the Ligands	5
Computational Study	7
Transient Absorption Time Profiles for ZnL1 in MeCN (N ₂)	10
Transient Absorption Time Profiles for ZnL2 in MeCN (N ₂)	11
Transient Absorption of ZnL1 in MeCN (O ₂)	12
Transient Absorption of ZnL2 in MeCN (O ₂)	14
Singlet Oxygen Spectra for Formation Yield Determination	16
Pulse Radiolysis Approach for the Generation of the Triplet State of ZnL1 and ZnL2	17
References	22

Description of the Crystal Structure of ZnL1

Recrystallization of ZnL1 from a mixed MeCN/CH₂Cl₂ solution provided single crystals of [(ZnL₁)₂]·2CH₂Cl₂·4MeCN suitable for X-ray crystallographic analysis. Crystals of [(ZnL₁)₂]·2CH₂Cl₂·4MeCN are monoclinic, with the space group *P*2₁/*n*. The asymmetric unit contains one half of the molecules of the formula unit. In contrast to the structure described below, here the solvate molecules were found to be heavily disordered and attempts to model the disorder were unsuccessful. On these grounds, the corresponding was removed from the structure (and the corresponding *F*₀) with the SQUEEZE algorithm implemented in the PLATON program suite.¹ The structure of the centrosymmetric ZnL2 complex is shown in Figure S11 along with selected bond lengths and angles. As can be seen, two supporting ligands wrap around two zinc atoms to give a helical structure encumbering a central cavity that is believed to host MeCN solvate molecules as found in the structure described below. The other solvate molecules occupy presumably the calix[4]arene cavities and other interstitial voids in the structure. The Zn ions are four-coordinated being surrounded by two imine N and two phenolato O atoms from L1 in a distorted tetrahedral that is one Zn atom exhibit a Λ-configuration and the other the enantiomeric Δ-configuration. The zinc atoms are coplanar with the chelate rings. The average Zn-O^{sal} and Zn-N^{sal} distances at 1.916(1) and 2.009(2) Å show no unusual features and compare well with those of other Zn(II) salicylaldiminato complexes.² The complex can be regarded as a double-stranded helix with a meso-configuration.

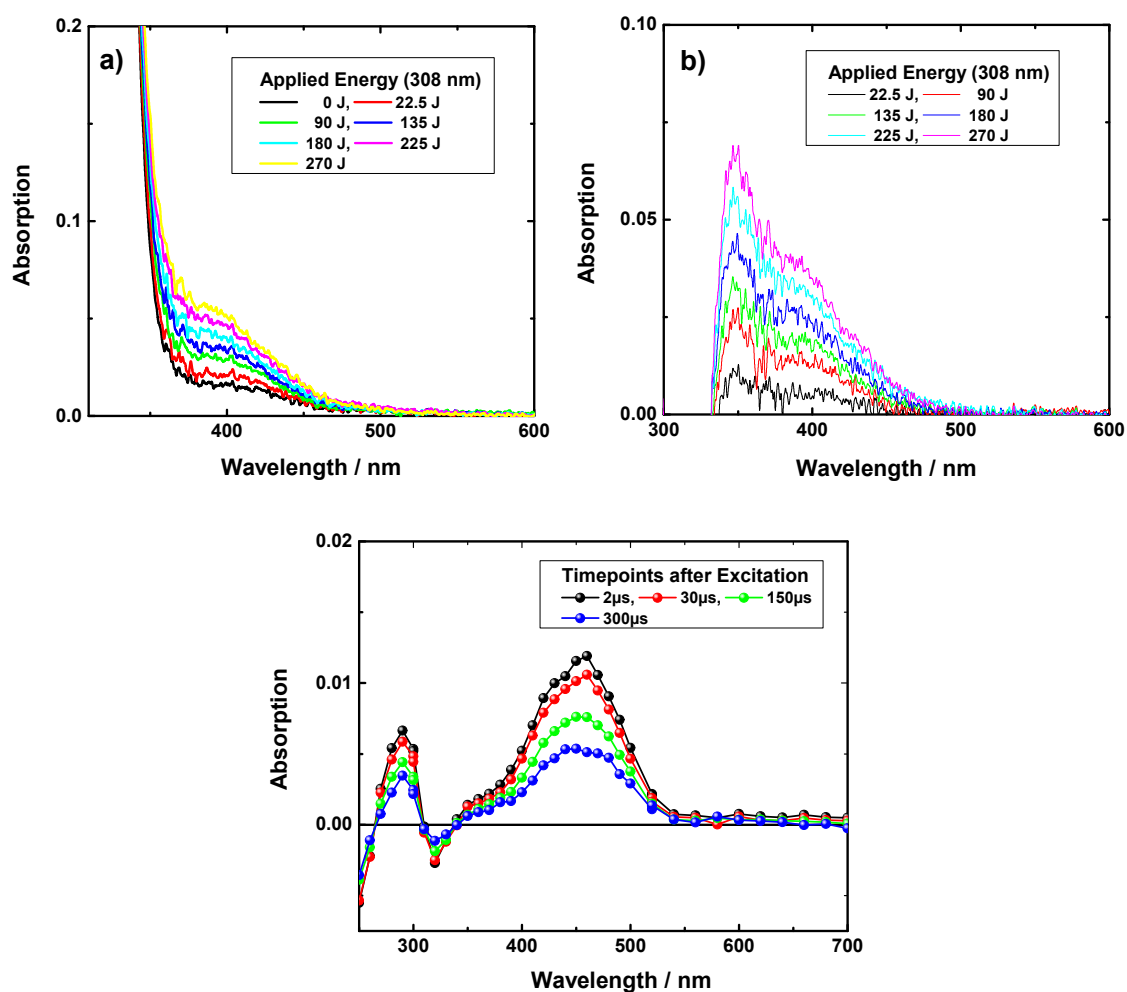


S11 Ball and stick representation of the molecular structure of the **ZnL1** complex in crystals of $[(\text{ZnL}^1)_2] \cdot 2\text{CH}_2\text{Cl}_2 \cdot 4\text{MeCN}$ as determined by single crystal X-ray diffraction. Selected bond lengths [Å] and angles [°]: Zn1-N1 2.011(2), Zn1-N2 2.006(3), Zn1-O5 1.920(2), Zn1-O6 1.912(2); O1...O2 2.76, O3...O4 2.71, Zn1...Zn1' 8.823; N1-Zn-N2 120.2(1), O5-Zn-N1 96.1(1), O5-Zn-N2 115.1(1), O5-Zn-O6 116.0(1), O6-Zn-N1 114.7(1), O6-Zn-N2 96.2(1). Symmetry code used to generate equivalent atoms: 1-x, 1-y, 1-z (').

Crystal Data for $[(\text{ZnL}^1)_2] \cdot 2\text{CH}_2\text{Cl}_2 \cdot 4\text{MeCN}$. $\text{C}_{92}\text{H}_{80}\text{N}_4\text{O}_{12}\text{Zn}_2$, $M_r = 1564.42$ g/mol, monoclinic, space group $P2_1/c$, $a = 13.9774(4)$ Å, $b = 19.5368(5)$ Å, $c = 18.3255(4)$ Å, $\beta = 103.656(2)$, $V = 4862.7(2)$ Å³, $Z = 4$, $\rho_{\text{calcd}} = 1.068$ g/cm³, $T = 180(2)$ K, $\mu(\text{Cu K}\alpha) = 1.187$ mm⁻¹ ($\lambda = 1.54186$ Å), crystal size $0.20 \times 0.20 \times 0.10$ mm³, 48899 reflections measured, 9166 unique, 6594 with $I > 2\sigma(I)$. Final $R_1 = 0.0689$ ($I > 2\sigma(I)$), $wR_2 = 0.1956$ (9166), 498 parameters, no restraints, min./max. residual electron density = $-0.53/0.98$ e/Å³.

Investigations on the Photoinduced Isomerisation of the Ligands

As discussed in the main text the photoexcitation of L1 and L2 results in the formation of a transient with slow relaxation rates in μs time range (figure 5 and SI2c). The transient was related to the photo induced isomerisation of L1 or L2. In order to further proof this relation to the photo isomerisation and exclusion of photo degradation we performed an experiment where the photoinduced degradation of L1 was induced on purpose. Therefore, a solution of L1 in MeCN ($A_{308\text{nm}} = 0.75$) was illuminated applying deep UV light $\lambda_{\text{ill}} = 308 \text{ nm}$, (0 – 128 J). The resulting UV-Vis spectra after different energy input are illustrated in figure SI2a. The absorption spectra of the photoproduct (SI2b) was estimated out of the difference between the absorption spectra of the non-illuminated and the illuminated sample. The photoproduct spectra show the formation of peak maximum around 400 nm. This illustrates a significant difference to the observed transient absorption spectra after excitation of L1 with 355 nm (SI2c). Regarding the transient absorption decay related to the back-isomerisation a homogeneous decay over the whole transient absorptions spectra was observed. Therefore, it can be concluded that transient absorption spectra observed in figure 5 and SI2c are mainly related to the formed isomer transient. As a consequence, the transient absorption decay might illustrate the back-isomerisation to the cis enol isomer. Note, small rates of photo degradation can not be fully excluded for high excitation pulse energies.



S12 a) UV-Vis spectra of a L1 solution in MeCN illuminated with 308 nm at different applied energy's, b) differential UV-Vis spectra received by subtracting the UV-Vis spectra of non-illuminated L1 from the illuminated L1 samples illustrated is the influence of different applied energy, c) Transient absorption spectra for different time spots after excitation of L1 in MeCN excited with 355 nm (5 mJ).

Computational Details

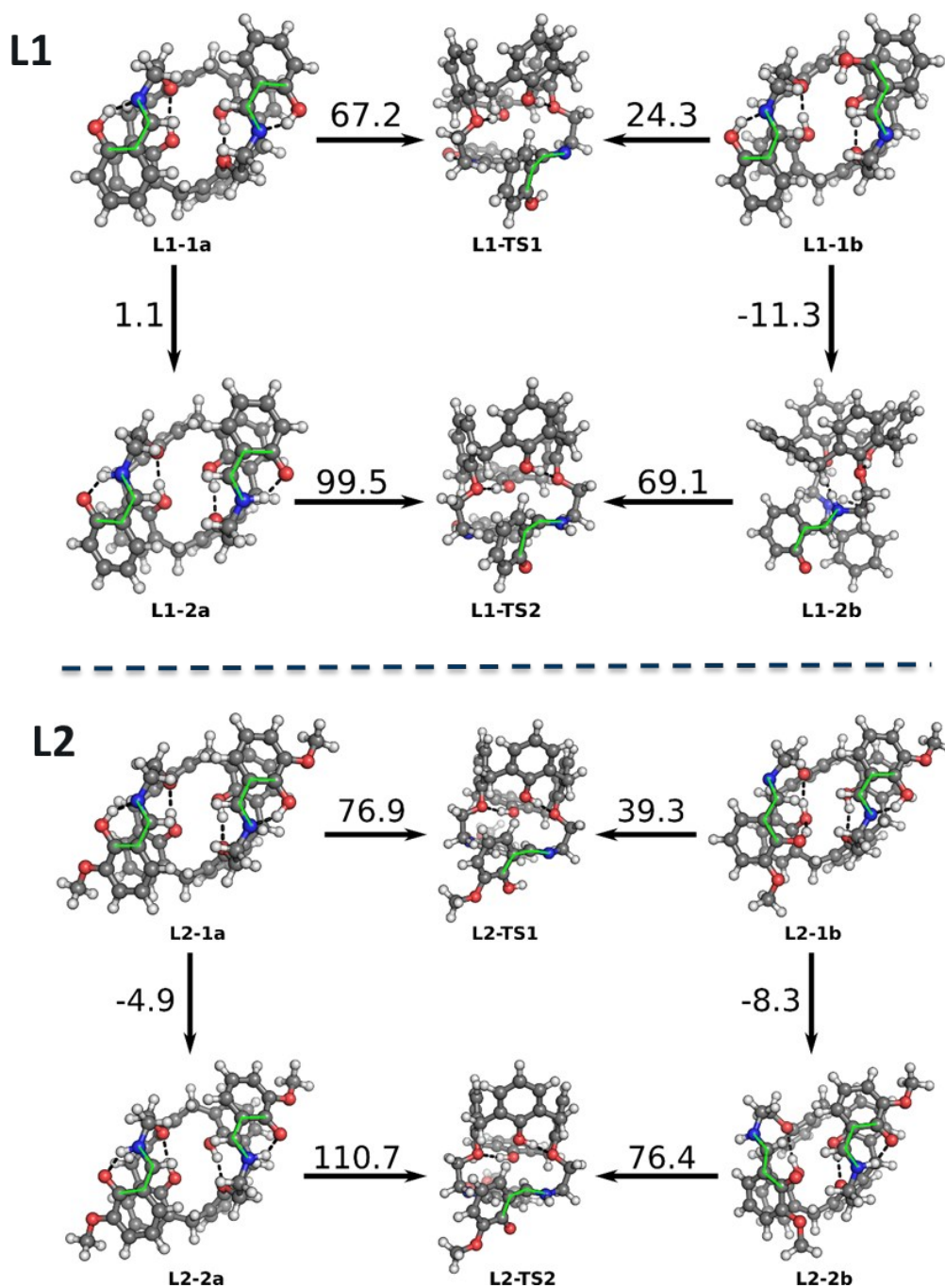
Gibb free Energy for the Isomerisaion process of L1 and L2

The Gibbs free energy of the cis and trans configuration of the enol and keto isomer, as well as the activation energy for the cis trans configuration change were calculated by applying DFT calculations (as described in the method part) for L1 (upper figure) and L2 (below figure). For each ligand system, the upper line represents the calculation for the enol isomer form as denoted by the insert 1. The left side represents the cis configuration as denoted by the letter a, the right side shows the trans configuration highlighted by the letter b. TS denotes the transition state configuration between the cis and the trans configuration. The arrow labels represent the difference of free Gibbs energy (kJ/mol) between the two connected structures.

The following conclusions can be derived from the calculations:

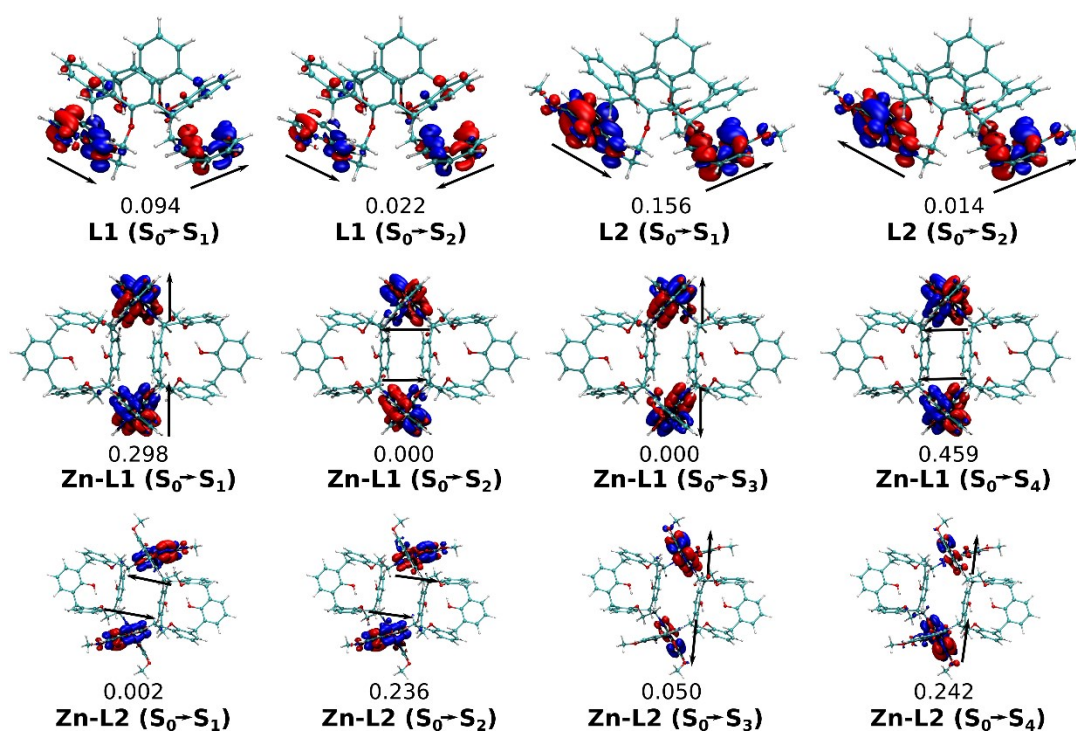
- For the cis configuration, the energy difference between the keto and enol form is rather small and within the error range of the method.
- There is a significant energy barrier between the cis and the trans configuration where the cis form is significantly more stable.
- In case of L2, the methoxy group substitution leads to a stabilisation of the keto cis-form compared to the enol-cis form. Furthermore, the activation barrier for the rotation from -trans to the -cis form is slightly increased.

These result are well in line with the experimental findings of the isomerisation and the possibility of back-isomerisation and the observed slower back-isomerisation kinetic for L2.



S13 DFT calculations results for the Gibbs free energy of the cis and trans configuration of the enol and keto isomer of L1 and L2, as well as the activation energy for the cis trans configuration change, all values in kJ/mol; L1-1a cis enol form of L1, L1 TS1 transition state between cis and trans enol form of L1, L1-1b trans configuration of the enol isomer of L1, L1-1b cis keto form of L1, L1 TS2 transition state between cis and trans keto form of L1, L1-1b trans configuration of the keto isomer of L1; L2-1a cis enol form of L2, L2 TS1 transition state between cis and trans enol form of L2, L2-1b trans configuration of the enol isomer of L2, L2-1b cis keto form of L2, L2 TS2 transition state between cis and trans keto form of L2, L2-1b trans configuration of the keto isomer of L2.

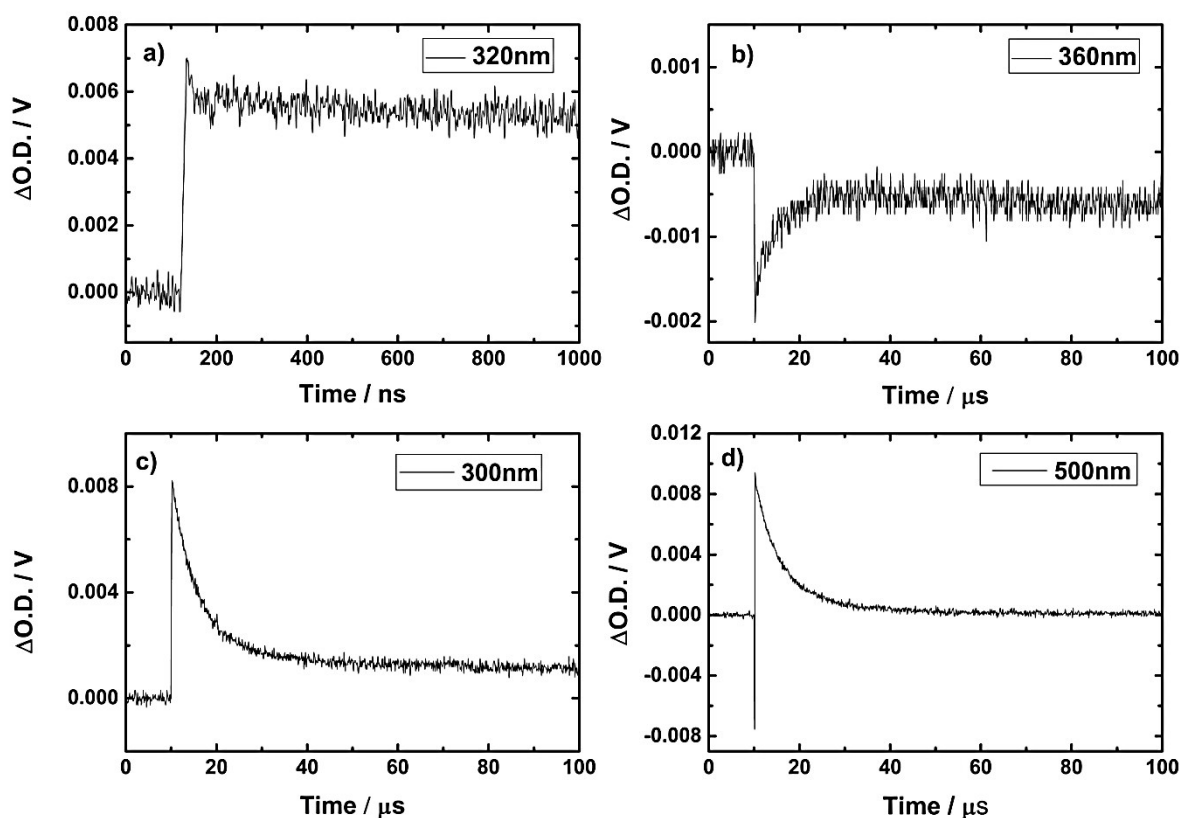
Oscillator strength and transition densities calculation for L1, L2, ZnL1 and ZnL2



SI4 Calculated oscillator strength and transition densities for shown ligands and complexes (method: CAM-B3LYP/def2-SVP/TDA). The black arrows illustrate orientation of local dipoles.

A comparison of the transition density for the investigated ligands reveals that the extension by the methoxy group increases the locale transition dipole moment at each salicylaldimine subunit, see SI4. This results in a stronger total oscillator strength for the $S_0 \rightarrow S_1$ transition since the dipole at each salicylaldimine subunit point into a similar direction (black arrows in SI4). After complexation with Zn, the alignment of the transition dipole moments is improved and the oscillator strength is increased further for the transitions where the local dipoles point into a similar direction ($S_0 \rightarrow S_1$ and $S_0 \rightarrow S_4$ for Zn-L1, $S_0 \rightarrow S_2$ and $S_0 \rightarrow S_4$ for Zn-L2). Please note, all excitations for the same ligand/complex in SI4 possess nearly the same energy, and thus, contribute to the first absorption band in the UV-Vis-spectra.

Transient Absorption Time Profiles for ZnL1 in MeCN (N₂)

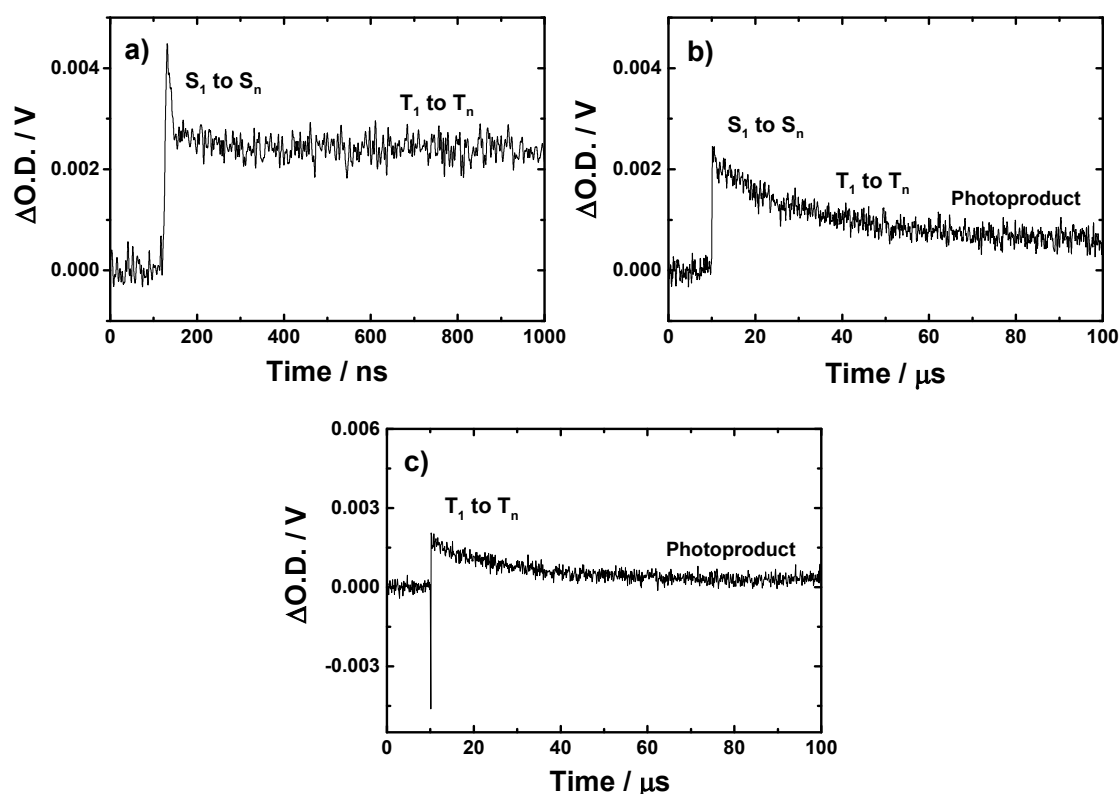


S15 Time profiles for the transient decay after excitation of ZnL1 ($\lambda_{ex} = 355$ nm, nitrogen atmosphere) for different probe wavelengths and time ranges: a) 320 nm, 1 μs ; b) 360 nm, 100 μs ; c) 300 nm, 100 μs ; d) 500 nm, 100 μs .

S15 depict the transient absorption decay at characteristic wavelength and time ranges of ZnL1 in MeCN, excited with $\lambda_{ex}=355$ nm and a pulse energy of 6mJ. Figure S15a shows the transient absorption decay at $\lambda = 320$ nm within a time range up to 1 μs . Note the excitation occurs at $t = 120$ ns. The time profile is based on the overlap of fast transient absorption decay directly after excitation and a slow incomplete decay. The fast decay belongs to the singlet state transient absorption and the slow decay can be related to the triplet state decay. Note, there is an overlap with the small transient absorption of the formed photoproduct. The Figures S15b-d illustrate the transient absorptions decays of the triplet state and the photoproduct at different wavelengths (300 nm, 360 nm and 500 nm). The transient absorption decays illustrate the relation of the triplet state and the permanent absorption of the formed photoproduct. An observation of the singlet state transient absorption decay is not possible

for figure SI5b-c due to the chosen time resolution. Note, the negative $\Delta O.D.$ in figure SI5b for $\lambda = 360$ nm is related to ground state bleaching.

Transient Absorption Time Profiles for ZnL2 in MeCN (N₂)

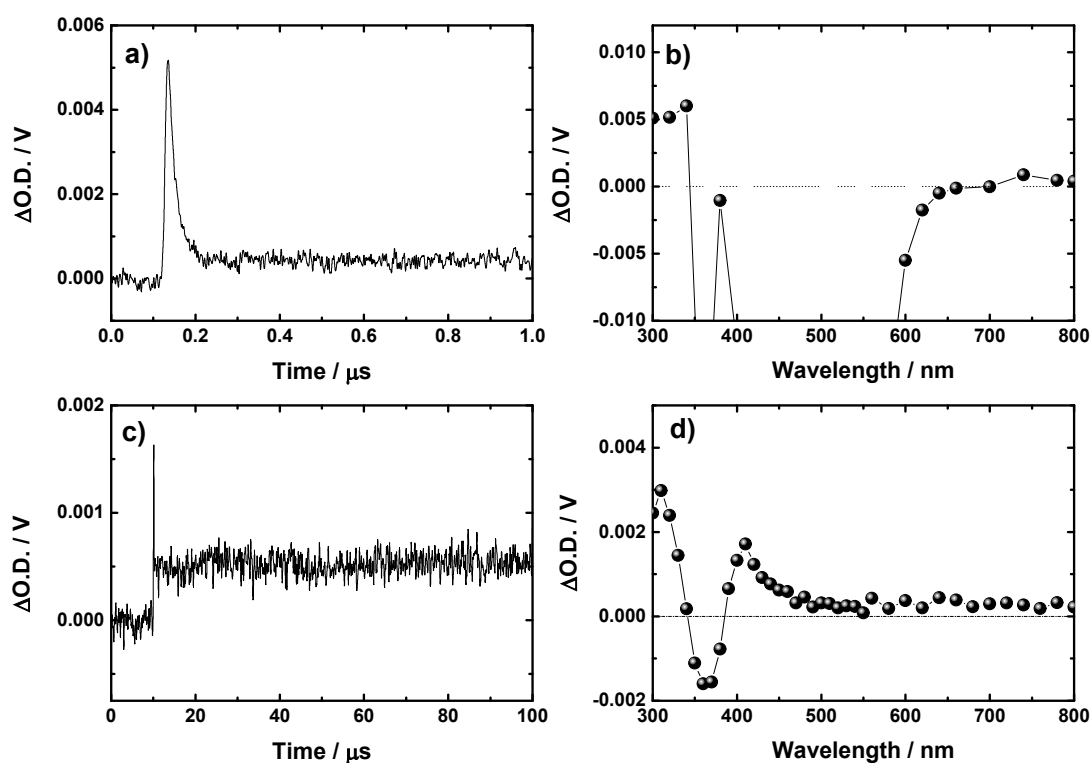


SI6 Time profiles for the transient decay after excitation of ZnL2 ($\lambda_{ex} = 355$ nm, nitrogen atmosphere, 6 mJ) for different probe wavelengths and time ranges: a) 320 nm time range 1 μs ; b) 320 nm time range 100 μs ; c) 520 nm time range 100 μs .

SI6 depict the transient absorption decay for characteristic wavelength and time ranges of ZnL2 in MeCN excited with $\lambda_{ex} = 355$ nm with a pulse energy of 6 mJ. Figure SI6a shows the transient absorption decay at $\lambda = 320$ nm within a time range up to 1 μs , excitation occurs at $t_{ex} = 120$ ns. The time profile correspond to the overlap of a fast transient absorption decay directly after excitation and a slow incomplete decay, well in line the results for ZnL1 (SI6a). The fast decay belongs to the singlet state transient absorption and the slow decay can be

related to the triplet state decay. Note, there is an overlap with the small transient absorption of the formed photoproduct by analogy with ZnL1. The figures SI6b-c illustrate the transient absorptions decays of the triplet state and the photoproduct at different wavelengths. An observation of the singlet state transient absorption decay is not possible for figure SI6b-c due to the chosen time resolution. Compared to ZnL1, the longer lifetime of the triplet state of ZnL2 is clearly observable. The less pronounced occurrence of ground state bleaching (not illustrated) is the result of the wavelength shift of the ground state and triplet state in case of ZnL2.

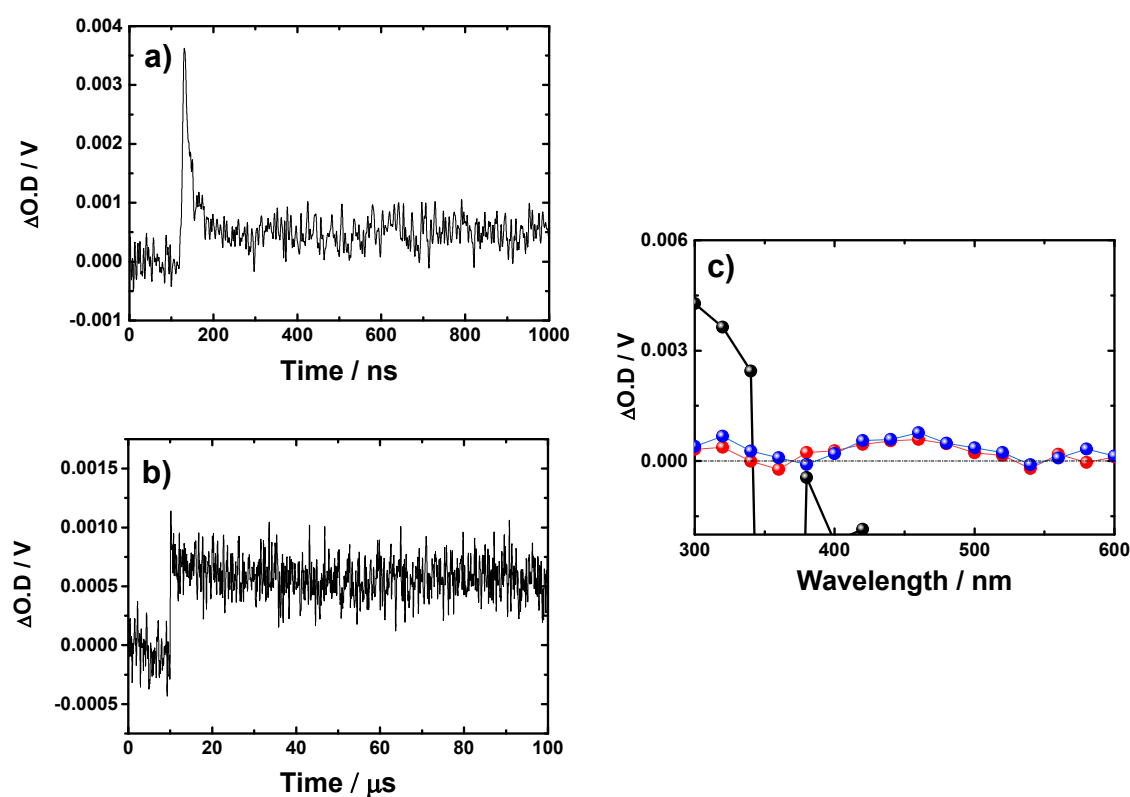
Transient Absorption of ZnL1 in MeCN (O_2)



SI7 Transient absorption behaviour of ZnL1 in MeCN after excitation ($\lambda_{ex} = 355$ nm, 5 mJ) under oxygen atmosphere: a) Transient absorption time profile 320 nm time range up to 1 μs ; b) Transient absorption spectra (300 – 800) nm for time point 5 ns after excitation; c) transient absorption time profile 320 nm time range up to 100 μs ; d) Transient absorption spectra (300 – 800) nm for time point 85 μs after excitation.

In order to exclude the triplet state related transient absorption spectra measurement in oxygen atmosphere were performed. Due to strong oxygen quenching rates the triplet state is completely quenched, enable the observation of the singlet state and the photoproduct related transient absorption bands. Figure SI7a-d illustrates distinctive transient absorption time profiles and transient absorption spectra of ZnL1 in MeCN under oxygen atmosphere after laser excitation with $\lambda_{\text{ex}} = 355 \text{ nm}$, 5mJ. Figure SI7a depict the time profile of the transient absorption decay at 320 nm for time ranges up to 1 μs where the excitation was triggered at $t_{\text{ex}} = 120 \text{ ns}$. The time profile is dominated by a fast decay related to the S_1 to S_n transition overlapping with a small $\Delta\text{O.D.}$ offset related to the formation of the photoproduct. Deconvolution of the excitation laser pulse (pulse width 6 ns) revealed a singlet state lifetime of about 8 ns. The difference between this result and the previous reported fluorescence lifetime (5.3 ns) can be related to the different excitation source and experimental conditions, as well as small effects of the photoproduct on the fit procedure. The related transient absorption spectra for $t = 5 \text{ ns}$ after the onset for the excitation is shown in figure SI7b. The spectrum is dominated by the fluorescence features ranging for 400 nm to 600 nm. The negative $\Delta\text{O.D.}$ around 355 nm can be related to an artefact of the excitation. The small transient absorption ranging from 340 nm to 300 nm is related to the S_1 to S_n transition. Note, the S_1 to S_2 transition is assumed to overlap with the fluorescence signal. The transient absorption time profile and spectra of the photo product are illustrated in figure c and d. The time profile at 320 nm (up to 100 μs , excitation at $t = 10 \mu\text{s}$) depict the weak permanent offset that indicates the formation of a stable photoproduct. Note, in order to have comparable results between the transient absorption in nitrogen and oxygen the pulse energy was not increased over 6 mJ per pulse and concentration ($c = 4 \cdot 10^{-5} \text{ M}$) even if the signal to noise ratio was low (15 accumulation per wavelength). Regarding the transient absorption spectra the lower signal to noise ratio makes it difficult to determine a clear transient absorption spectra. Nevertheless, the spectra can be interpreted to exhibit two main peaks. The first one ranges from 300 nm to 340 nm and the second one from 400 nm to 550 nm, well in line with the results of the transient absorption of L1.

Transient Absorption of ZnL2 in MeCN (O₂)



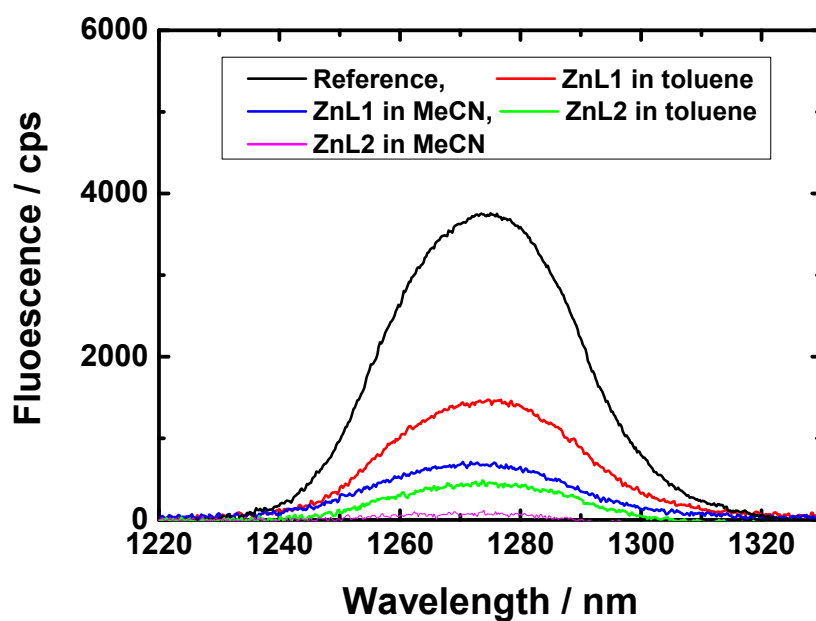
S18 Transient absorption spectra of ZnL2 in MeCN after excitation upon 355 nm under oxygen atmosphere: a) Transient absorption time profile 320 nm time range up to 1 μs ; b) Transient absorption time profile 320 nm time range up to 100 μs ; c) Transient absorption spectra (300 – 800) nm at different time spot after excitation: 5 ns (black), 6.5 μs (red), 90 μs (blue).

In Figure 8-c the transient absorption time profiles and transient absorption spectra of ZnL2 in MeCN under oxygen atmosphere after laser excitation with $\lambda_{ex} = 355$ nm, 6 mJ per pulse are illustrated. Figure S18a depicts the time profile of the transient absorption decay at 320 nm for the time ranges up to 1 μs (excitation occurred at $t = 120$ ns). The time profile is dominated by a fast decay related to the S_1 to S_n transition overlapping with a small $\Delta O.D.$ offset related to the formation of the photoproduct. This is in well agreement to the results for ZnL1. Deconvolution of the excitation laser pulse (pulse width 6 ns) revealed a singlet state lifetime of about 3 ns that is also slightly longer than the previous reported fluorescence lifetimes. Note, a similar behaviour was observed for ZnL1. For the time range up to 100 μs (excitation

at $t = 10 \mu\text{s}$) a permanent offset indicates the formation of a stable photoproduct (SI8b). The corresponding transient absorption spectra for $t = 5 \text{ ns}$, $6.5 \mu\text{s}$ and $90 \mu\text{s}$ after the excitation are illustrated in figure SI8c showing the transient absorption of the singlet state and the photoproduct, respectively. The transient spectra at $t = 5 \text{ ns}$ depict similar features as observed for ZnL1: a dominating fluorescence ranging for 400 nm to 600 nm, a negative $\Delta\text{O.D.}$ around 355 nm caused by the excitation and a small transient absorption ranging from 340 nm to 300 nm related to the S_1 to S_n transition. The transient absorption behaviour of the photoproduct is represented by the transient absorption spectra at later time points ($t = 6.5 \mu\text{s}$ and $t = 90 \mu\text{s}$), where two main transient absorption peaks are observable. The first peak ranges from 300 to 340 nm. The second transient absorption ranges from 400 to 550 nm with local maxima around 450 nm. Therefore, the observed transient absorption of the photoproduct formed after excitation of ZnL2 is comparable to the transient absorption of the photoproduct formed after excitation of L2. This evidences that the photodegradation is not totally suppressed by the zinc complexation. This issue will be addressed by investigating further improvement of the ligand design in subsequent works.

Singlet Oxygen Spectra for Formation Yield Determination

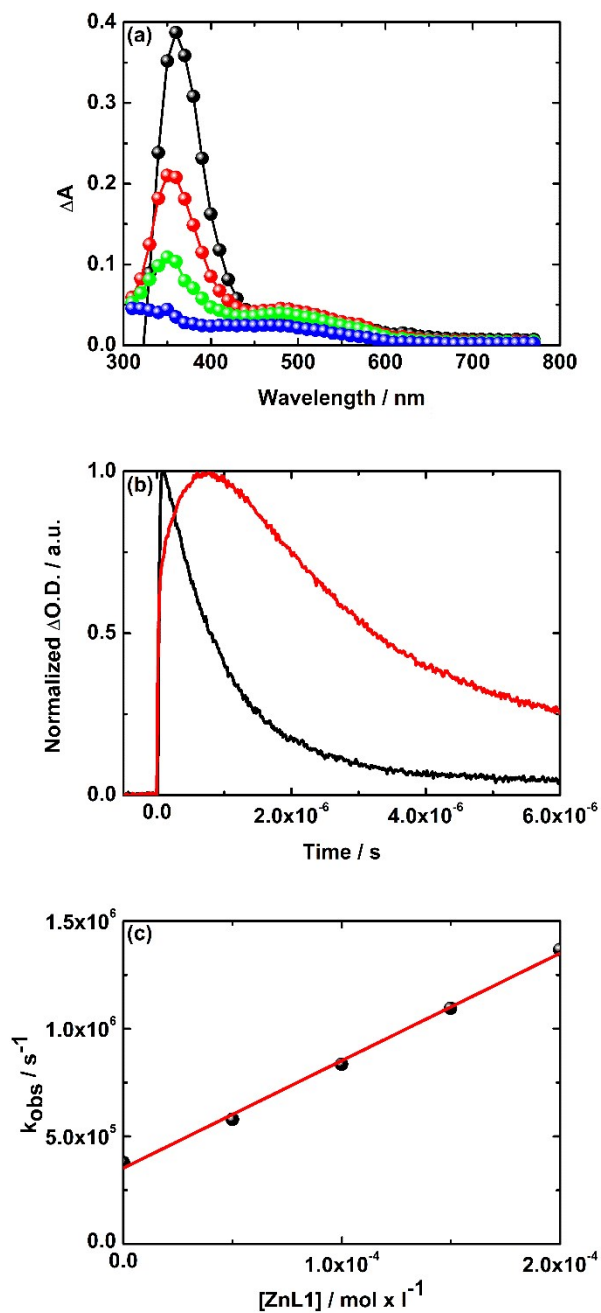
Figure S19 illustrates selected spectra of the singlet oxygen phosphorescence achieved after excitation of the photosensitizer (ZnL1 and ZnL2 or MPC60) in different solvents MeCN and toluene. Even if the spectra were not normalized to the corresponding absorption value, the trend of different singlet oxygen yields discussed in the main text is already obvious.



S19 Determination of the singlet oxygen formation, luminescence spectra of singlet oxygen formation after excitation ($\lambda_{\text{ex}} = 350 \text{ nm}$) of: MPC60/reference in MeCN, $A = 0.06$ (black); ZnL1 in toluene, $A = 0.16$ (red); ZnL1 in MeCN, $A = 0.075$ (blue); ZnL2 in toluene, $A = 0.13$ (green); ZnL2 in MeCN, $A = 0.22$ (magenta).

Pulse Radiolysis Approach for the Generation of the Triplet State of ZnL1 and ZnL2

In order to determine the triplet extinction coefficients and the quantum yield a pulse radiolysis approach was investigated as described in the main text. In the following we will demonstrate the result for the pulse radiolysis of ZnL1 (Figure SI10) representative for both ZnL1 and ZnL2. The applied spectra and time profiles for the determination of the extinction coefficients and triplet yields are then represented in figure SI10 – SI12. The pulse radiolysis experiments were performed using nitrogen saturated toluene solutions containing $5 \cdot 10^{-2}$ M Biphenyl (BPh) and between 0.5 and $2 \cdot 10^{-4}$ M ZnL1. The triplet transient absorption of BPh with its characteristic transient absorption maximum around 360 nm was observed shortly after the electron pulse (see figure SI10).³ This transient absorption decayed rapidly and gave rise to a new set of transient absorption bands (see SI10b) in the UV and visible part of the optical spectrum with a discernible band in the visible maximizing around 480 nm. The rate constant for the energy transfer from the BPh triplet state (^3BPh) to ZnL1 was determined via the analysis of the plot of the pseudo-first order rate constant obtained from the mono-exponential fits of the 360 nm time absorption profiles versus the ZnL1 concentration, as shown in figure SI10c. A linear relationship between the observed pseudo-first order rate constant and the ZnL1 concentration was found. From the slope of the linear fit, a rate constant for the energy transfer of $k_{\text{ENT}} = 5 \cdot 10^9 \text{ M}^{-1} \cdot \text{s}^{-1}$ was determined.



SI10 a) Pulse radiolysis (85 Gy/pulse, 10 ns FWHM) transient absorption spectra from a N_2 saturated toluene solution containing $5 \cdot 10^{-2}$ M BPh and $1.5 \cdot 10^{-4}$ M ZnL1, 100 ns (black), 700 ns (red), 1.5 μ s (green) and 3 μ s (blue) after the electron pulse. b) Corresponding normalized absorption time profiles at 360 nm (black) and 480 nm (red). c) Corresponding plot of the pseudo-first-order rate constants taken from the 360 nm time profiles vs. the ZnL1 concentration.

The extinction coefficient of the energy donor (^3BPh), the intrinsic decay constant k_0 for ^3BPh under our conditions, the energy transfer rate constant k_{EnT} and the absorption spectrum of **ZnL1** were used to determine the triplet-triplet absorption spectrum of **ZnL1** including a kinetic correction⁴ taking the competition between the energy transfer to **ZnL1** versus the decay of ^3BPh into the ground state into account:

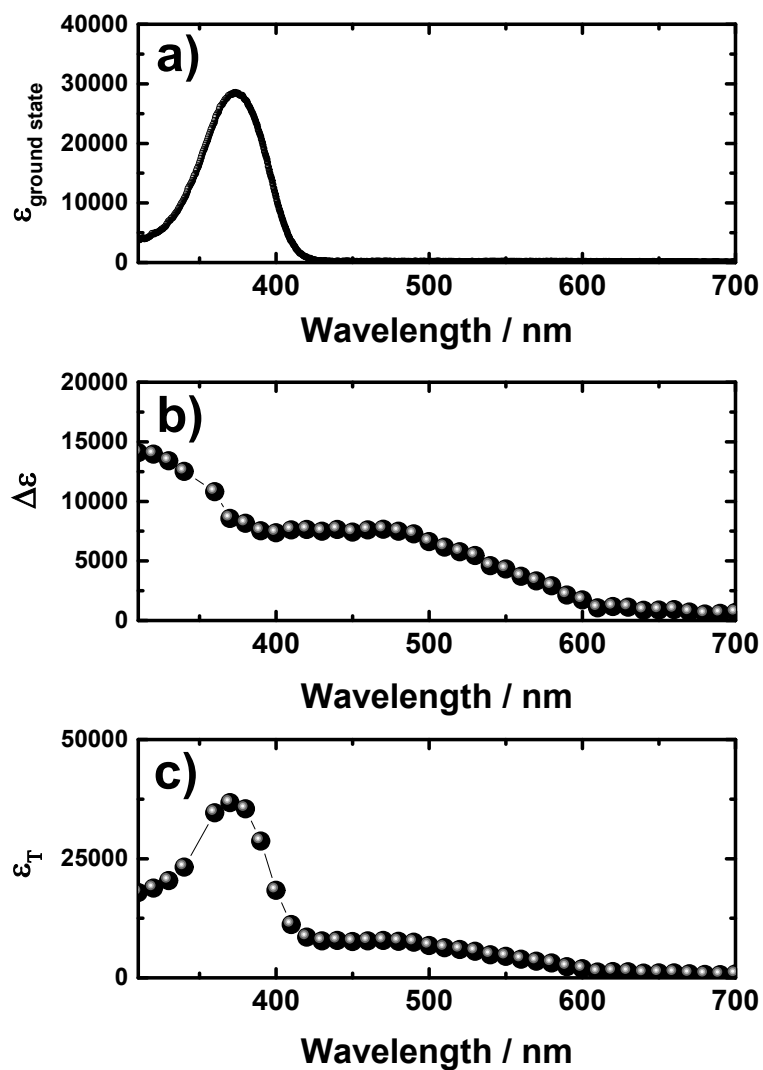
$$\frac{1}{\Delta A_{\text{ZnL1}}} = \left(\frac{\Delta \varepsilon_{3^* \text{BPh}}}{\Delta \varepsilon_{3^* \text{ZnL1}} * \Delta A_{3^* \text{BPh}}} \right) \left(1 + \frac{k_0}{k_{\text{EnT}} * [\text{ZnL1}]} \right) \quad (1)$$

ΔA_{ZnL1} and $\Delta A_{3^* \text{BPh}}$ are the maximum changes in the optical absorption of ^3BPh and $^3\text{ZnL1}$ with $\Delta \varepsilon_{3^* \text{ZnL1}}$ and $\Delta \varepsilon_{3^* \text{BPh}}$ as the extinction coefficients difference at the wavelengths of relevance. This is 360 nm for ^3BPh since for this wavelength the extinction coefficient is known. For $^3\text{ZnL1}$ 530 nm was selected as there is no overlap by the transient absorptions of ^3BPh . Plotting $1/\Delta A_{\text{ZnL1}}$ versus $1/[\text{ZnL1}]$ gives a linear relation and the intercept of the linear fit is $\Delta \varepsilon_{3^* \text{BPh}} / (\Delta \varepsilon_{3^* \text{ZnL1}} * \Delta A_{3^* \text{BPh}})$. Substituting $\Delta \varepsilon_{3^* \text{BPh}}$ with $27000 \text{ M}^{-1} \text{ cm}^{-1}$ and $\Delta A_{3^* \text{BPh}}$ with 0.4 we obtain a value of around $5400 \text{ M}^{-1} \text{ cm}^{-1}$ for $\Delta \varepsilon_{3^* \text{ZnL1}}$ at 530 nm.

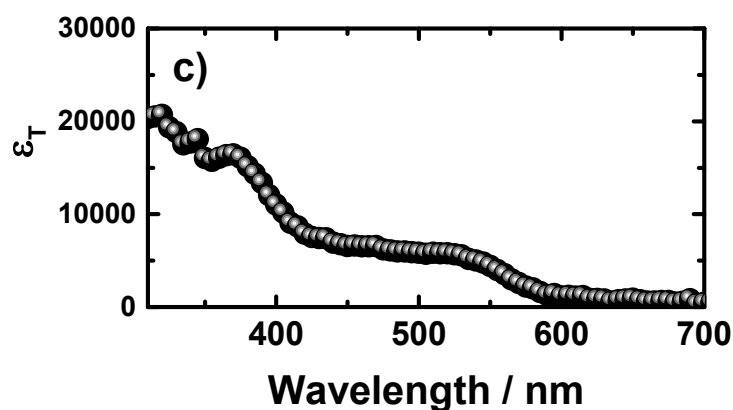
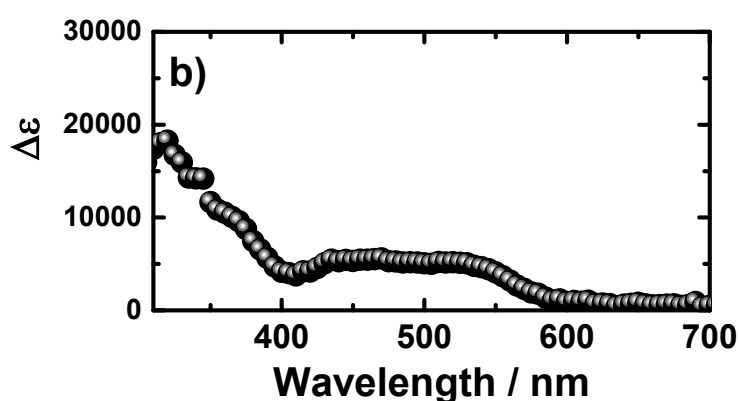
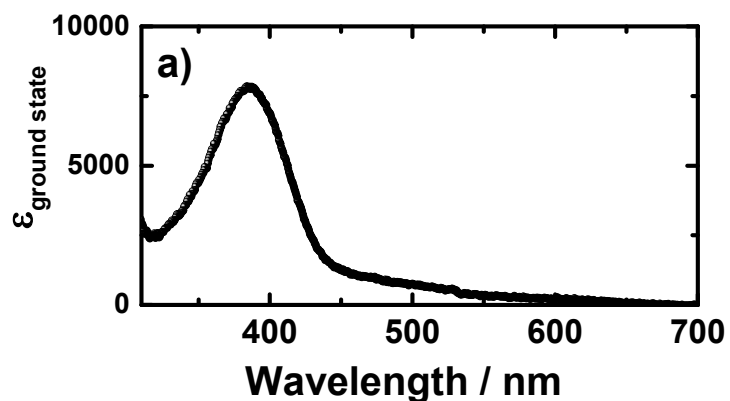
With this value the transient absorption spectrum of $^3\text{ZnL1}$ was rescaled yielding a $\Delta \varepsilon$ spectrum for $^3\text{ZnL1}$ (SI11b). The addition of the ground state extinction coefficients spectrum ε_{GS} (SI11a) is correcting for underlying ground state bleaching due to ground state absorption and gives the $^3\text{ZnL1}$ spectrum in extinction coefficients ε_{T} as depicted in figure SI11c calculated by:

$$\varepsilon_{\text{T}} = \Delta \varepsilon + \varepsilon_{\text{GS}} \quad (2)$$

The same approach was used for the determination of the triplet extinction coefficient of ZnL2 (Figure 11 a-c).



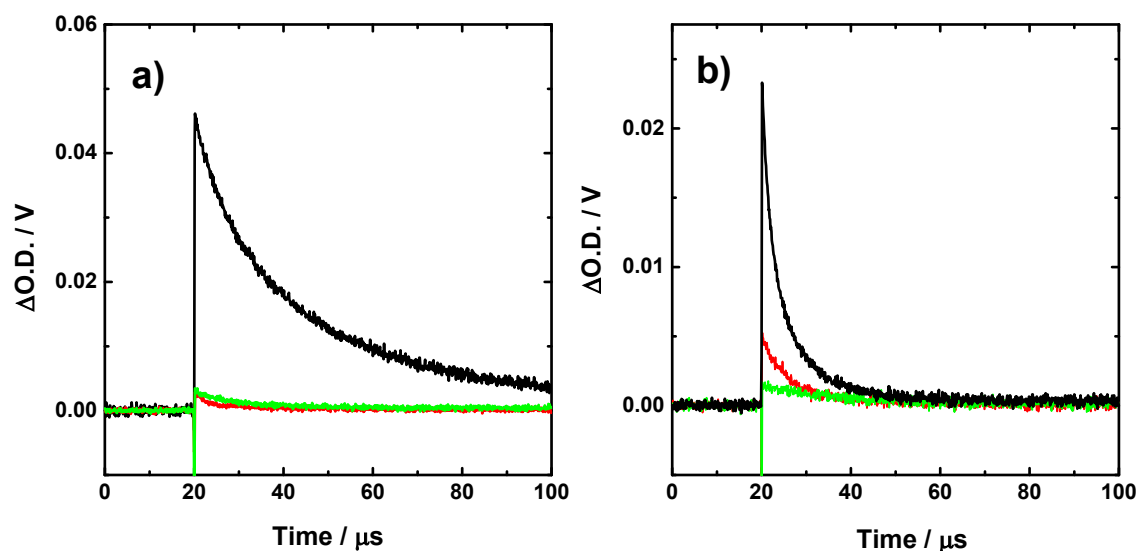
S111 a) Absorption spectra of ZnL1 ($c = 2.2 \cdot 10^{-5}$ M) in toluene; b) $\Delta\epsilon$ against wavelength plot established out of the transient absorption spectra of the pulse radiolysis experiment ($t = 5 \mu\text{s}$, 85 Gy / pulse); c) calculated ϵ_T against wavelength plot.



SI12 a) Absorption spectra of ZnL2 ($c = 3.1 \cdot 10^{-5}$ M) in toluene; b) $\Delta\epsilon$ against wavelength plot established out of the transient absorption spectra of the pulse radiolysis experiment ($t = 5 \mu\text{s}$, 85 Gy/pulse); c) calculated ϵ_T against wavelength plot.

Applying the extinction coefficients of ZnL1 and ZnL2, the quantum yields in toluene and MeCN, as well as extinction coefficients in MeCN were calculated using reference molecules with well-known photophysical properties as discussed in the main text. Herein, the $\Delta\text{O.D.}$ values of ZnL1 and ZnL2 in toluene and MeCN were directly compared to the $\Delta\text{O.D.}$ values of the reference materials. Anthracene was used as reference in toluene and benzophenone in

MeCN. The applied transient absorption time profiles can be seen in figure SI13a,b. The black colour transient absorption time profiles are related to the reference material, the red to ZnL1 and the green time profile to ZnL2. Note, for the chosen probe wavelength a negligible transient absorption of the photoproduct can be expected.



SI13 Applied transient absorption time profiles for determining the triplet quantum yield and extinctions coefficient of ZnL1 and ZnL2; a) Anthracence, $\lambda = 428$ nm (black), ZnL1, $\lambda = 500$ nm (red), ZnL2, $\lambda = 500$ nm (green) in toluene; b) Benzophenone $\lambda = 520$ nm (black), ZnL1, $\lambda = 500$ nm (red), ZnL2, $\lambda = 520$ nm (green) in MeCN

References

- 1 P. van der Sluis and A. L. Spek, *Acta Cryst. A*, 1990, **46**, 194.
- 2 A.-C. Chamayou, S. Lüdeke, V. Brecht, T. B. Freedman, L. A. Nafie and C. Janiak, *Inorg. Chem.*, 2011, **50**, 11363.
- 3 Y.H. Meyer, R. Astier and J.M. Leclercq, *Chem. Phys. Lett*, 1970, **4**, 587.
- 4 I. Carmichael and G. L. Hug, *J. Phys. Chem. Ref. Data*, 1986, **15**, 1.